EXPERIMENTAL AND COMPUTATIONAL STUDIES ON L – PROLINIUM PICRATE

[1]R.Subaranjani, [1]M.Victor Antony Raj, [1]S.Prathap*
[1]Department of Physics, Loyola College, Chennai-600 034

Abstract : New organic NLO materials are most needed in the field of Laser and technology. Experimental authentication for theoretical predictions is an important scenario in the field of research. L – PROLINIUM PICRATE (LPOP) is a new NLO material synthesized and grown as good quality single crystal. LPOP molecule is simulated using Gaussian 09 software package and its structural, Vibrational, First order Hyperpolarizability the HOMO-LUMO gap are calculated then the results are compared with experimentally obtained values. It is found that LPOP crystallizes in monoclinic system with $P2_1$ space group. Theoretically calculated Bond lengths and angles coincide well with experimentally obtained results. The Vibrational assignment for the functional groups of the molecule proves the structural stability of the molecule. The first order hyperpolarizability of LPOP is calculated as 9.567007 x 10^{-30} esu and the calculated energy value of HOMO - LUMO gap is found to be -0.1943 a.u (5.287 eV).

I. INTRODUCTION

Amino acid crystals usually display large nonlinear optical (NLO) response and are potential candidates for applications in the emerging areas of photonics [1]. Molecules that show asymmetric polarization induced by electron donor and acceptor groups are responsible for electro optic and NLO properties [2].Over the past two decades much attention has been paid to the search of novel high quality NLO materials that can generate high second order optical nonlinearities [3,4,5]. Organic NLO materials are formed by weak Van der Waals and hydrogen bonds with conjugated π electrons and are more advantageous than their inorganic counterparts due to high conversion efficiency for second harmonic generation and transparency in the visible region, high resistance to optical damage and so on. They also offer the flexibility of molecular design and the promise of virtually an unlimited number of crystalline structures. Traditionally, crystals of organic materials have been grown from the melt or from vapor or solution.

In the present work, an attempt is made to synthesize and grow a NLO material L-Prolinium Picrate (LPOP) using L-Proline and Picric acid. The LPOP crystals grown by slow evaporation are characterized by powder XRD, and molecular simulation. The theoretical values were compared with the experimental values using Gaussian 03.

2. EXPERIMENTAL PROCEDURE

L-Prolinium Picrate is synthesized from equimolar solution of L - Proline and Picric acid by slow evaporation. The solubility data was determined by dissolving the synthesized salt of LPOP in 100 ml of mixed solvent of double distilled water and acetone at a constant temperature. The solubility of LPOP increases with the temperature and thus exhibit positive solubility coefficient. The solubility curve is as shown in Fig 1 Transparent yellow color single crystals were obtained from the re-crystallization salt. Seed crystal is then placed in its supersaturated solution kept in a bath at ambient temperature. Seed crystals are grown to big crystals by slow evaporation to a size of about 14 x 2 x3 $mm^3$with good transparency in a time of about ten days (Fig.2).

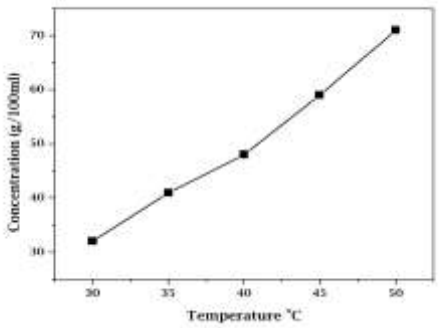

Fig 1 Solubility curve of LPOP

Fig 2 Photograph of as grown LPOP single crystal

3. RESULTS AND DISCUSSION

3.1 Single crystal XRD Analysis

In order to obtain the crystal data of LPOP crystals, single crystal X-ray diffraction studies were carried out using ENRAF NONIUS CAD4-F single crystal X-ray diffractometer with MoKα radiation (λ=0.71073 Å) radiation. The single crystal XRD data of LPOP crystal indicates that it Monoclinic system with a = 10.908 (3) Å, b= 5.353 (2) Å, c= 12.476 (5) Å and β=109.141 (4) the space group being $P2_1$ with a volume of 688.21 (4) $Å^3$. The crystal data and structural refinement data are given in Table 1.

3.2 Powder X-ray diffraction analysis

In addition to single crystal XRD data, powder X-ray diffraction analysis was also carried out for the identification of the synthesized crystal using an X-ray diffractometer, MODEL RICH SEIFERT, XRD 3000P with monochromatic nickel filtered Cu K_α (λ = 0.15406 nm) radiation. The sample was scanned over the range 10 - 40° at the rate of one degree/minute. The spectrum recorded at room temperature is depicted in Fig 3. Theoretically Simulated XRD pattern of LPOP single crystal is given in Fig 4. Both XRD patterns are almost similar in comparison.

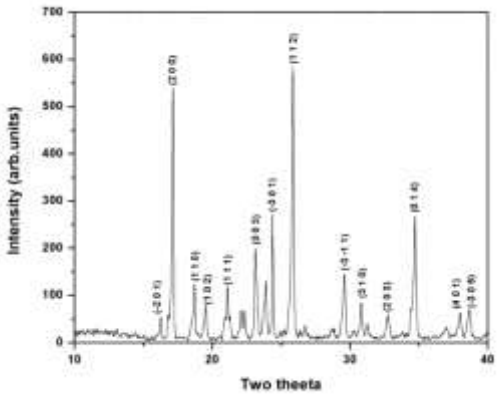

Fig 3. Experimentally obtained powder XRD pattern of LPOP

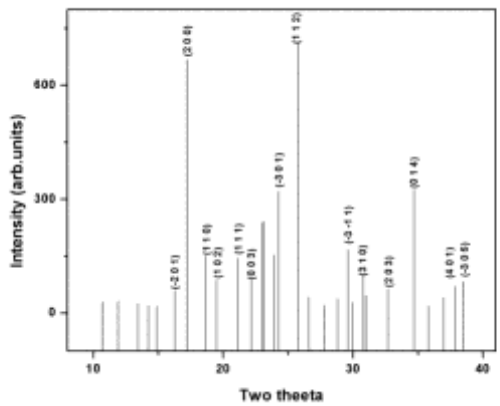

Fig 4. Theoretically simulated powder XRD pattern of LPOP

Table 1 Crystal parameters of LPOP

Empirical Formula	$C_{11}H_{12}N_4O_9$	
Formula weight	344.25 g/mol	
Wave length	0.71073 Å	
Crystal system, Space group	monoclinic, $P2_1$	
Unit cell dimensions	a =10.908Å b =5.353Å c =12.476 Å	α = γ = 90° β = 109.141°
Cell volume	688.21 $Å^3$	

3.3 Computational Details

The molecular structure optimization of the title compound and corresponding vibrational harmonic frequencies were calculated using the Density Functional Theory with Beckee-3-Lee-Yag-Parr (B3LYP) combined with 631G (d, p) basis set.

The fundamental vibrational frequencies, IR intensity and force constants were calculated using the Gaussian 03 package [6]. By combining the results of the GAUSSVIEW program with symmetry considerations, vibrational frequency assignments were made with a high degree of accuracy. The defined coordinate form complete set and matches quite well with the motions observed using GAUSSVIEW program.

Molecular Geometry

The molecular structure along with numbering of atoms of LPOP is as shown in Fig. 5. The most optimized structural parameters were calculated and were depicted in Table 2 and 3.

Vibrational Analysis

The vibrational spectroscopy has been extensively used to understand the factors contributing to linear electro-optic effect from the vibrational modes in organic materials and to provide deeper knowledge regarding intermolecular interactions, relationship between molecular architecture, non-linear response and hyperpolarizability. The present work describes the vibrational spectral studies of LPOP molecule. In order to qualitatively analyze the presence of functional groups in LPOP, FT-IR spectrum of the grown crystal was recorded in the range 500 cm^{-1} to 4000 cm^{-1}, using KBr pellet technique on BRUKER IFS FT-IR Spectrometer. Recorded FT-IR spectrum of the LPOP molecule is shown in Fig 6. The optimized structural parameters also used to compute the vibrational frequencies of the stable isolated molecule of LPOP at DFT using B3LYP/6-31G (d,p) level of calculations. The normal modes of LPOP are distributed amongst the symmetry species as there are 102 normal modes of fundamental vibrations which span the irreducible representations. Γ_{N-6} = 69 A′ (in-plane) + 33 A″ (out-of-plane) respectively.

All the vibrations are active in Infrared vibrations. Selected fundamental modes of vibrational assignments with the observed and calculated frequencies of LPOP molecule is reported in Table 4.

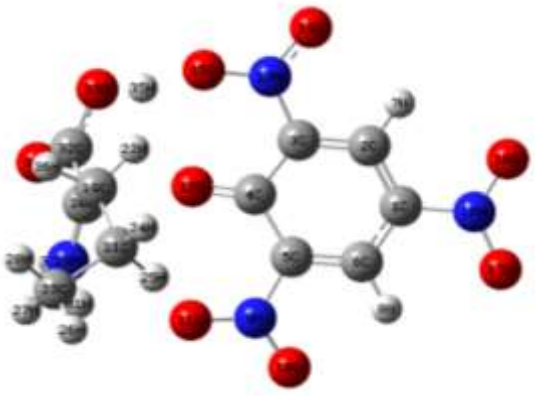

Fig 5 Atomic numbering system adapted for ab initio computations of LPOP molecule

Table 2 Selected bond lengths of LPOP molecule

Atoms	Gaussian(Å)	XRD(Å)
C_1-C_2	1.39202	1.39061
C_2-C_3	1.39010	1.38775
C_3-C_4	1.45726	1.45502
N_{16}-O_{17}	1.26682	1.26919
N_{16}-O_{18}	1.26615	1.26847
C_3-N_{13}	1.44059	1.44014
N_{29}-H_{30}	1.01743	1.01351
N_{29}-H_{31}	1.01322	1.01035
O_{33}-H_{35}	1.00498	0.99793
C_{23}-H_{27}	1.09677	1.09231

Table 3 Selected bond angles of LPOP molecule

Atoms	Gaussian(˚)	XRD(˚)
C_1-C_2-C_3	119.55744	119.56879
C_2-C_3-C_4	122.86610	122.87786
C_3-C_4-C_5	113.29239	113.24049
C_1-N_{16}-O_{17}	117.86289	117.98683
C_1-N_{16}-O_{18}	118.02602	118.14247
C_2-C_3-N_{13}	116.52505	116.79101
O_{10}-N_9-O_{11}	122.61956	122.50704
C_{19}-C_{21}-C_{23}	114.67571	114.57703
N_{29}-C_{20}-C_{32}	114.09023	114.53278
O_{34}-C_{32}-O_{33}	124.20885	123.95991
C_{32}-O_{33}-H_{35}	117.33103	117.64071
H_{30}-N_{29}-H_{31}	117.84107	117.49813

O–H Vibrations

The O–H group gives rise to three vibrations (stretching, in-plane bending and out-of-plane bending vibrations). The O–H group vibrations are likely to be the most sensitive to the environment, so they show pronounced shifts in the spectra of the hydrogen bonded species. The hydroxyl stretching vibrations are generally observed in the region around 3500cm^{-1} [7]. In the case of the un-substituted phenols it has been shown that the frequency of O–H stretching vibration in the gas phase is 3657 cm^{-1}[8]. Similarly in our case a very strong FT-IR band at 3778 is assigned to O–H stretching vibration. The O–H in-plane bending vibration in the phenols, in general lies in the region 1150–1250cm^{-1} and is not much affected due to hydrogen bonding unlike to stretching and out-of-plane bending frequencies. In our present investigations strong band observed in FT-IR spectrum at 703 cm^{-1} is assigned to O–H out-of-plane bending vibration.

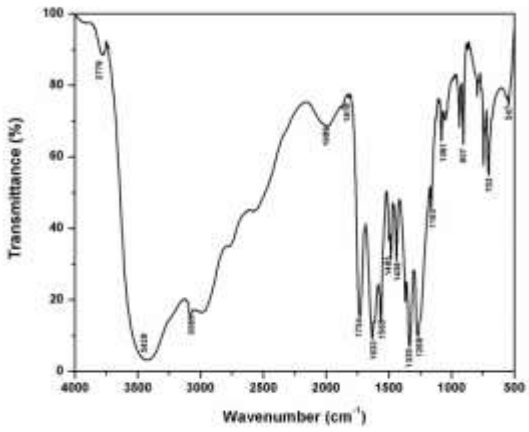

Fig 6. Experimentally obtained FT-IR spectrum of LPOP

Table 4 Selected Vibrational Assignments of LPOP Molecule

No	Frequency cm^{-1}		Spectroscopic assignment	Force constant	Reduced mass
	B3LYP	Experimental			
102	3905.7095	-	OH st	9.5792	1.0658
95	3743.5770	3778	OH st	9.0229	1.0928
91	3440.0117	3428	NH st	7.2622	1.1049
85	3073.0714	3085	CH st	6.1311	1.1019
63	1650.3371	1633	C=N st	5.3319	3.3227
60	1582.3453	1565	NH_2sci	1.5411	1.0447
54	1485.5051	1483	CH ipb	1.5349	1.1805
49	1412.1045	1438	CH_3sydef	1.5353	1.3068
42	1326.6140	1335	CO st	1.3617	1.3132
37	1223.0089	1268	CO st	1.6858	1.9129
34	1108.3035	1163	CN st	1.6637	2.2988
28	1036.4037	1031	CH d	1.3715	2.1672
21	904.7890	907	CH d	0.6088	1.2622
16	723.4959	703	O-H opb	1.1482	3.7230
11	545.6198	547	CN ipd	1.3247	6.5561
1	78.3285	-	CNH_2 t	0.0091	2.5121

St-stretching;sci-scisorring; t-twisting; ipb-in-planebending; opb- out-of-plane bending;ipd-inplane deformation; sydef – symmetric deformation; d –deformation

C-N Vibrations

The C-N ring stretching vibration bands occur in the region 1600 - 1500 cm^{-1} [9]. The present molecule exhibits this vibration in IR spectrum at 1633$cm^{-1}$and the theoretically computed value at 1650cm^{-1} by B3LYP method shows good agreement with recorded spectrum. C–N stretching absorption assigned in the region 1382–1266 cm^{-1} [10]. In the present work, the band observed at 1163 cm^{-1} in FT-IR spectrum has been assigned to C–N stretching vibration.

C-O Vibrations

The C-O stretching vibration for this molecule is obtained at 1335 and 1268cm^{-1} in IR spectrum. Both the bands well coincided with theoretically calculated values at 1326 and 1223 cm^{-1} using B3LYP method.

3.4. Hyperpolarizability studies

The force exerted by the molecular packing and intermolecular interactions in the crystal will play as a decisive factor for the determination of macroscopic properties of these materials. So, understanding these intermolecular interactions should help towards understanding the nature of the macroscopically produced effects. The ab initio calculated non-zero μ value shows that this compound might have microscopic first static hyperpolarizabilities with non-zero values obtained by the numerical second-derivative of the electric dipole moment according to the applied field strength. The magnitude of molecular hyperpolarizability, presence of the number of chromophores and the degree of noncentrosymmetry are the deciding criteria of the second order susceptibility $\chi^{(2)}$ values in an NLO system. A large value of the first hyperpolarizability is the prerequisite to behave as a good NLO material, and the important parameters influencing β generally are (i) donor–acceptor system, (ii) nature of substituents, (iii) conjugated π system and (iv) the influence of planarity.

As mentioned above, this study is extended to the determination of the electric dipole moment μ_{tot}, the isotropic polarizabilityα_{tot} and the first hyperpolarizability β_{tot} of the title compound. It is well known that the nonlinear optical response of an isolated molecule in an electric field $E_i(\omega)$ can be presented as a Taylor series expansion of the total dipole moment, μ_{tot}, induced by the field:

$$\beta_{tot} = \mu_0 + \alpha_{ij}E_j + \beta_{ijk}E_jE_k + \cdots \quad (1)$$

where μ_0 the permanent dipole moment, α_{ij} is the linear polarizability and β_{ijk} is the first hyperpolarizability tensor components. The isotropic (or average) linear polarizability is defined as[11] (Zhang et al 2004)

$$\beta_{tot} = \frac{\alpha xx + \alpha yy + \alpha zz}{3} \quad (2)$$

First hyperpolarizability is a third rank tensor that can be described by 3×3×3matrix. The 27 components of 3D matrix can be reduced to 10 components due to the Kleinman symmetry[12] (β_{xyy}, β_{yxy}, β_{yyx}, β_{yyz}, β_{yzy}, β_{zyy},. . . likewise other permutations also take same value). The output from Gaussian 03 provides 10 components of this matrix as β_{xxx}, β_{xxy}, β_{xyy}, β_{yyy}, β_{xxz}, β_{xyz}, β_{yyz}, β_{xzz}, β_{yzz}, β_{zzz}, respectively. The components of the first hyperpolarizability can be calculated using the following equation [13].

$$\beta_i = \beta_{iii} + \frac{1}{3}\Sigma_{i\neq j}(\beta_{ijj} + \beta_{jij} + \beta_{jji}) \quad (3)$$

Using the x, y and z components of β, the magnitude of the first hyperpolarizability tensor can be calculated by:

$$\beta_{tot} = (\beta_x^2 + \beta_y^2 + \beta_z^2)^{1/2} \quad (4)$$

The complete equation for calculating the magnitude of β from Gaussian 03 output is given as follows:

$\beta_{tot} = ((\beta_{xxx} + \beta_{xyy} + \beta_{xzz})^2 + (\beta_{yyy} + \beta_{yzz} + \beta_{yxx})^2 + (\beta_{zzz} + \beta_{zxx} + \beta_{zyy})^2)^{1/2}$ (5)

The total static dipole moment μ, the mean polarizabilityα_o, the anisotropy of the polarizability$\Delta\alpha$ and the mean first hyperpolarizability β_o, using the x, y, z components they are defined as

$\mu=(\mu_x^2 + \mu_y^2 + \mu_z^2)^{1/2}$ (6)

$\alpha_o=(\alpha_{xx}+\alpha_{yy}+\alpha_{zz})^{1/3}$ (7)

$\beta_o=(\beta_x^2 + \beta_y^2 + \beta_z^2)^{1/2}$ (8)

The first order hyperpolarizability (β_{ijk}) of LPOP is calculated using 6-31G(d,p) basis set based on finite field approach. The calculated first order hyperpolarizability values for LPOP molecule are given in Table 5.

3.5. HOMO-LUMO Gap

It is understood from the Molecular theory that the interaction between HOMO and LUMO produces π-π* transition an essential behavior for NLO molecules. Therefore, HOMO energy is directly related to ionization potential, LUMO energy is directly related to the electron affinity. Energy difference between HOMO and LUMO orbital is called as energy gap that is an important stability for structures. In the present study HOMO-LUMO energy gap for LPOP molecule is calculated and the plot is shown in Fig 7. The calculated energy value of HOMO - LUMO gap is found to be -0.1943 a.u (5.287 eV) this explains the eventual charge transfer interaction within the molecule which influences the first order hyperpolarizabilities.

Table 5 Hyperpolarizability of LPOP in esu

Hyperpolarizability in esu	
β_{xxx}	839.381487
β_{xxy}	409.551019
β_{xyy}	101.669540
β_{yyy}	83.295976
β_{xxz}	-458.15500
β_{xyz}	122.412637
β_{yyz}	-21.110807
β_{xzz}	-1.1272407
β_{yzz}	147.024591
β_{zzz}	596.746509
β_{tot}	9.567007×10^{-30}

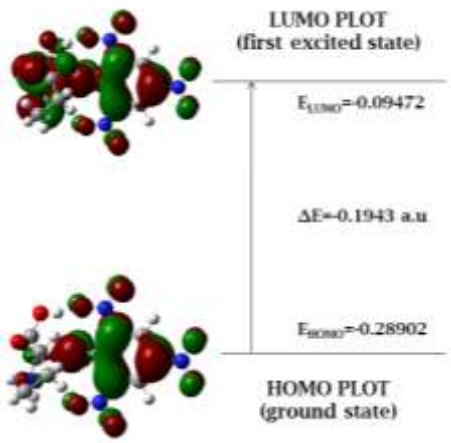

Fig 7 HOMO–LUMO plot of LPOP molecule

4. CONCLUSIONS

Single crystals of LPOP are conveniently grown by employing slow evaporation technique in a period of ten days. Powder XRD studies show that the grown crystal belongs to monoclinic crystal system having non-centrosymmetry with $P2_1$ space group. Optimized structure of the isolated LPOP molecule obtained by DFT calculations give the minimum energy state. Existence of strong hydrogen bond in the donor accepter coupling was understood from bond lengths. First order hyperpolarizability of LPOP is calculated and it is found useful in molecular designing. Theoretical and experimental Spectroscopic studies exemplify the presence of various functional groups in the molecule. Both theoretically simulated and experimentally obtained FT-IR spectra show coincidence. A frontier molecular orbital analysis gives the HOMO-LUMO energy gap value.

Reference

[1]. Badan J, R. Hierle, A. Perigaud, American Chemical Society, Washington, 1993
[2]. Prasad P. N, DJ. Wollians, Introduction to Nonlinear Optical Effects 111, Molecules and Polymers, Wiley, New York, 1991.
[3]. Aggarwal M. D, Stephens J, J.Optoe1ectron.Adv.Mater 5 (2003) 3.
[4]. Razzetti, M. Ardoino, L. Zaotti, M. Zha, C. Parorici, Cryst. Res.Technol. 37 (2002) 456.
[5]. Dhanuskodi, J. Ramajothi, Cryst. Res. Technol. 39 (2004) 592.
[6]. Frisch M.J, Trucks G.W, Schlegel H.B, Scuseria G.E, Robb M.A, J.R. Cheeseman J.R, Montgomery Jr J.A, Vreven T, Kudin K.N, Burant J.C, Millam J.M, Iyengar S.S, Tomasi J, Barone V, Mennucci B, Cossi M, Scalmani G,.Rega N, Petersson G.A, Nakatsuji H, Hada M, Ehara M, Toyota K, Fukuda R, Hasegawa J, Ishida M, Nakajima T, Honda Y, Kitao O, Nakai H, Klene M, Salvador P, Dannenberg J.J, Zakrzewski V.G, Dapprich S, Daniels A.D, Strain M.C, Farkas O, Malick D.K, Rabuck A.D, Raghavachari K, Foresman J.B, Ortiz J.V, Cui Q, BaboulA.G, Clifford S, Cioslowski J, Stefanov B.B, Liu G, A.Liashenko, Piskorz P, Komaromi I, Martin R.L, Fox D.J, Keith T.,.Al-Laham M.A, Peng C.Y, Nanayakkara A, Challacombe M, Gill P.M.W, Johnson B, Chen W, Wong M.W, Gonzalez C, Pople J.A, Gaussian 03, Revision C.02, Gaussian Inc.,Wallingford, CT, 2004.
[7]. Sajan D, I. Hubert Joe, Jayakumar V S, Zaleski J., J. Mol. Struct., 785 (2006) 43.
[8]. Michalska D, D.C. Bienko, A.J.A. Bienko, Z. Latajka., J. Phys. Chem., 100 (1996) 1186.
[9]. Socrates G., Infrared and Raman Characteristic Group Frequency, third ed.,Wiley, New York, 2001.
[10]. Shanmugam, Sathyanarayana.,Spectrochim. Acta., 40A (1984) 757.
[11]. Zhang Yun, Hua Li, Bin Xi, YunxiaChe, JiminZheng , (2008) Materials Chemistry and Physics Vol. 108 (2008) 192–195.
[12]. Kleinman. D. A., Phys. Rev. 126 (1962) 1977.
[13]. Sun Y, X. Chen, L. Sun, X. Guo, W. Lu, J. Chem. Phys. Lett. 381 (2003) 397.